# Conceptual prediction of harbor sedimentation quantities using AI approaches to support integrated coastal structures management

Elnabwy, M. T., Elbeltagi, E., El Banna, M. M., Elsheikh, M. Y., Motawa, I., Hu, J. W., & Kaloop, M. R. (2022). Conceptual prediction of harbor sedimentation quantities using AI approaches to support integrated coastal structures management. *Journal of Ocean Engineering and Science*. Advance online publication. https://doi.org/10.1016/j.joes.2022.06.005



**Publication Status:**
Published online: 02/06/2022

**DOI:**
10.1016/j.joes.2022.06.005

**Document Version**
Version created as part of publication process; publisher's layout; not normally made publicly available

Journal of Ocean Engineering and Science xxx (xxxx) xxx

Contents lists available at ScienceDirect

Journal of Ocean Engineering and Science

journal homepage: www.elsevier.com/locate/joes

# Conceptual prediction of harbor sedimentation quantities using AI approaches to support integrated coastal structures management

Mohamed T. Elnabwy[a,b], Emad Elbeltagi[b], Mahmoud M. El Banna[a], Mohamed Y. Elsheikh[b], Ibrahim Motawa[b], Jong Wan Hu[c,d,*], Mosbeh R. Kaloop[d,e]

[a] *Coastal Research Institute, National Water Research Center, Alexandria 21415, Egypt*
[b] *Structural Engineering Department, Mansoura University, Mansoura 35516, Egypt*
[c] *Department of Civil and Environmental Engineering, Incheon National University, Incheon 22012, South Korea*
[d] *Incheon Disaster Prevention Research Center, Incheon National University, Incheon 22012, South Korea*
[e] *Public Works Engineering Department, Mansoura University, Mansoura 35516, Egypt*

ARTICLE INFO

*Article history:*
Received 25 November 2021
Revised 18 April 2022
Accepted 1 June 2022
Available online xxx

*Keywords:*
Sedimentation
Coastal modeling system (CMS)
Artificial intelligence (AI)
Integrated coastal structures management (ICSM)
Sensitivity analysis

ABSTRACT

Sedimentation is one of the most critical environmental issues facing harbors' authorities that results in significant maintenance and dredging costs. Thus, it is essential to plan and manage the harbors in harmony with both the environmental and economic aspects to support Integrated Coastal Structures Management (ICSM). Harbors' layout and the permeability of protection structures like breakwaters affect the sediment transport within harbors' basins. Using a multi-step relational research framework, this study aims to design a novel prediction model for estimating the sedimentation quantities in harbors through a comparative approach based on artificial intelligence (AI) algorithms. First, one hundred simulations for different harbor layouts and various breakwater characteristics were numerically performed using a coastal modeling system (CMS) for generating the dataset to train and validate the proposed AI-based models. Second, three AI approaches namely: Support Vector Regression (SVR), Gaussian Process Regression (GPR), and Artificial Neural Networks (ANN) were developed to predict sedimentation quantities. Third, a comparison between the developed models was conducted using quality assessment criteria to evaluate their performance and choose the best one. Fourth, a sensitivity analysis was performed to provide insights into the factors affecting sedimentation. Lastly, a decision support tool was developed to predict harbors' sedimentation quantities. Results showed that the ANN model outperforms other models with mean absolute percentage error (MAPE) equals 4%. Furthermore, sensitivity analysis demonstrated that the main breakwater inclination angle, porosity, and harbor basin width affect significantly sediment transport. This research makes a significant contribution to the management of coastal structures by developing an AI data-driven framework that is beneficial for harbors' authorities. Ultimately, the developed decision-support AI tool could be used to predict harbors' sedimentation quantities in an easy, cheap, accurate, and practical manner compared to physical modeling which is time-consuming and costly.



## 1. Introduction

Sedimentation is one of the most common environmental issues that concerns the maintenance of harbors' entrances. It decreases navigation depth and prevents the movement of boats so that dredging operations are necessary to preserve appropriate depths. The amount of dredged sediments is the highest costly item in harbor operational costs. For example, in Egypt, the annual dredging cost of Damietta harbor for the year 2014 was LE58.03 million for dredging 1.744 million $m^3$ from the inner basin of the harbor [1]. Therefore, taking this issue into consideration from the conceptual design is important to minimize sedimentation within harbors' basins. The major focus for decision-makers is to find a solution that achieves both environmental and economic objectives by allowing sufficient discharge through the harbor which will mitigate the sedimentation issue.

The amount of sedimentation found to be significantly influenced by the conditions of the harbor's layout, physical, and envi-

* Corresponding author at: Department of Civil and Environmental Engineering, Incheon National University, Incheon 22012, South Korea.
*E-mail address:* jongp24@inu.ac.kr (J.W. Hu).

https://doi.org/10.1016/j.joes.2022.06.005
2468-0133/

ronmental issues. The geometry of the harbor, which greatly influences the flow patterns within the harbor, plays a vital role in the sediment transport within the harbor's basin [2]. Also, in coastal modeling applications, coastal structures such as rubble mound breakwaters are often perceived as solid and impermeable structures. In fact, certain designs of rubble mound structures with a greater riprap in the core can result in a significant porosity of the structure that provides flow and sediment pathways that can destabilize breakwaters, trigger sediment accumulation in the navigation channel, and increase the cost of harbor maintenance [3]. Therefore, it is important to incorporate the structural properties of the breakwater (such as: riprap diameter, porosity, etc.) in coastal numerical modeling to simulate their effects on sediment transport within harbor basin.

In Egypt and worldwide, most preliminary feasibility studies for coastal structures are focused on environmental effects during the construction stage without taking into consideration other impacts that may be resulted during the operation stage such as sedimentation issues as reported in previous studies [4,5]. Furthermore, the lack of funding is a hindrance to construct physical models to study sedimentation issues in a practical manner. For this reason, Integrated Coastal Structures Management (ICSM) is required through sophisticated techniques such as numerical modeling and artificial intelligence (AI) approaches to better understand the processes affecting coastal structures to help both decision-makers and local communities make the right decision about the optimal forms, design, and management for harbors. As such, this study highlights this vital need to provide the Egyptian harbors' authorities with decision-support AI tools that can be used to provide an accurate prediction of sedimentation quantities.

### 1.1. Research background

In recent decades, several researchers have been seeking to analyze the deposition problems in the harbor entrance basins. Demirbilek et al. [6] suggested some engineering solutions such as constructing a dike to reduce the amount of sediment entering the Pascagoula harbor, USA. Yin et al. [7] performed an experiment on the sediments transport in square harbors to study the impact of tidal and steady currents in order to suggest some general requirements for improving the harbor flushing cycle and reducing dredging needs. Winterwerp [8] proposed case studies for sediment deposition control in harbor basins. Such improvements were accomplished by raising the exchange rate between harbor and surface water and by raising the accumulation of sediment in the water reaching the basin. Kuijper et al. [9] discussed the effect of harbor's layout on harbor basin sedimentation, along with the introduction of the Current Deflection Wall (CDW) as a method of spatial modification to mitigate accumulated sediment in the Hamburg harbor basin. Yüksek [10] performed an experimental analysis on the impact of breakwater configurations on sedimentation levels in harbor basins and proposed certain design criteria in the form of dimensionless breakwater geometric parameters. Stoschek and Zimmermann [11] published a comparative study of the effect of harbor's layout on the circulation of sediments in an estuarine tidal harbor. Van-Rijn [12] utilized the results of field observations and numerical modeling to analyze sedimentation in estuarine and propose solutions to mitigate this issue. Mojabi et al. [2] utilized 2D sediment transport model to analyze the influence of harbor layout on the transport of sediment within square harbors by adjusting entry locations and found that entry position did not significantly affect the suspended sediment exchange levels, entry locations near the basin corner which resulted in less sedimentation. Sakhaee and Khalili [13] utilized Mike's 21 hydrodynamic modules to investigate the impact of breakwater extension on sediment transport at Nowshahr port for decreasing sediment deposition rates within the port's basin in order to facilitate marine traffic and provide effective dredging programs. Li et al. [3] studied the sediment transport around the porous breakwater of the American Dana's harbor to reduce the required dredging costs. They firstly used Coastal Modelling System (CMS) to investigate numerically the effect of the breakwater's permeability on accumulated sedimentation within harbor basin. Then, the resulted sedimentation quantities from the CMS were compared against the accumulated sedimentation available from historical dredging records to validate the model results. Furthermore, CMS has proven to be a valuable numerical tool for estimating the harbors' sedimentation quantities [6,14].

Considering the preceding information, although various researchers have dealt with individual aspects of sedimentation issues such as harbor's layout and the breakwater's permeability, a comprehensive framework is still needed that integrates these aspects in a practical manner. As such, this research bridges this knowledge gap by studying the impact of both harbor's layout and breakwater's permeability to provide an accurate forecast for the Egyptian harbors' sedimentation quantities. Herein, from the presented literature, there are two approaches widely employed to forecast harbors basins' sedimentation, including numerical modeling and physical modeling. Out of these approaches, AI approaches include Support Vector Regression (SVR), Gaussian Processing Regression (GPR), Fuzzy logic (FL), Artificial Neural Networks (ANN), etc. These computing approaches were used in various fields to validate the outcome of physical and numerical studies that are time-consuming and costly [15–18]. Deshmukh et al. [19] combined the ANN and numerical approaches to predict wave height. Patil et al. [20] incorporated SVM and Genetic Algorithms (GAs) to predict the wave transmission through floating breakwaters based on experimental wave transmission data from regular wave flumes at marine structure laboratory. Furthermore, many hybrid models are utilized for modelling sedimentation issues and for many other applications [21–31]. However, to the best of the authors' knowledge, no AI approaches were used to study the sedimentation and to quantify the relationship between the whole physical parameters of harbors' basins and the accumulation of sedimentation. To this end, this study attempts to help harbors' authorities by developing an integrated data-driven decision-support tool based on AI approaches to accurately predict harbor sedimentation quantities to minimize the cost and time associated with constructing physical models.

### 1.2. Research significance and objectives

Numerous experimental and numerical efforts have been carried out in the literature to study sedimentation issues with some studies focus on the effects of harbors' layout [2,10,13]. Other studies focus on the effects of hydrodynamic forces [7,32] and other ones focus on the structural characteristics of structures (e.g., permeability of breakwaters) [3]. However, the sedimentation rates in harbors depend on the interaction of multiple factors such as harbors' layout with the associated structures characteristic, site condition (e.g., geological and geotechnical characteristics), and environment changes (e.g. due to natural causes, such as storm), or due to human intervention, (e.g., the construction of breakwaters and docks). Thus, it is difficult to have a general formulation that considers all the factors that influence the sedimentation rates. Therefore, this paper aims to develop an AI robust computational approach to study the impact of the possible aspects on the sedimentation process. Ezbet Elborg fishing harbor, Egypt, is used as a case study in the current development. The associated objectives of this study are:

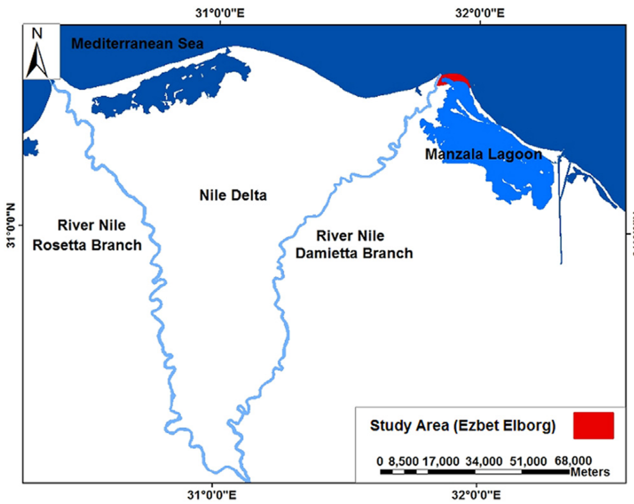


**Fig. 1.** The location of study area.

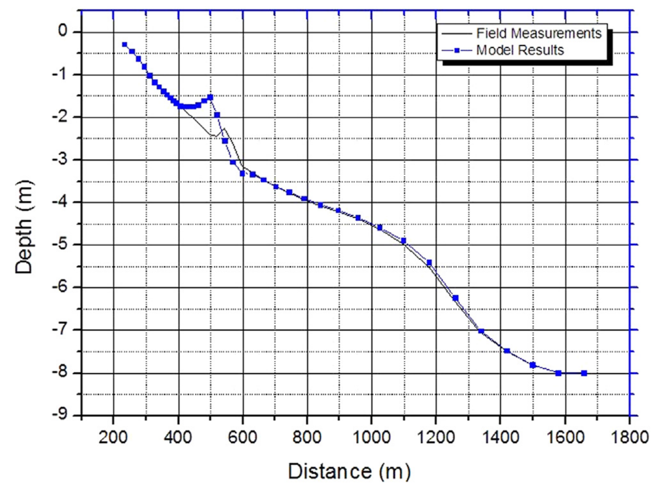


**Fig. 2.** Comparison between measured and modeled profile for the study area.

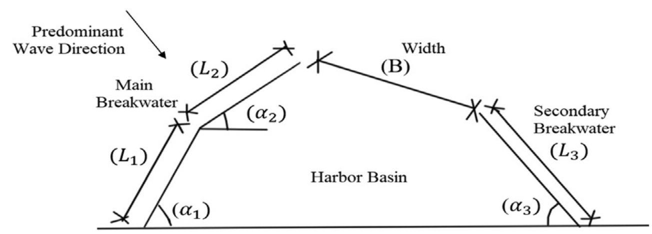


**Fig. 3.** Harbor geometry parameters.

(1) Investigating the effect of whole parameters on harbors' sedimentation by using 100 scenarios generated numerically by the CMS.
(2) Developing three AI approaches namely: SVR, GPR, and ANN for predicting the sedimentation quantities and evaluating their performance using various criteria such as the Root Mean Squared Error (RMSE), the Scatter index (SI) and the Coefficient of Correlation (CC).
(3) Conducting a sensitivity analysis to determine the effect of each single input parameter on sedimentation to minimize data space by neglecting input variables with low influence on the final outcomes of the developed AI model.
(4) Developing a graphical user interface (GUI) as a decision-making tool to be used by harbors' authorities for the management of harbors in Egypt with the ability to accurately predict the sedimentation quantities.

## 2. Study area

Ezbet Elborg city (Fig. 1) located on the Nile's Delta NE coast where 60% of all Egyptian fishing activities exist [33]. The Egyptian government seeks to construct a new fishing harbor east of this coastal city for solving the problems of fishermen. Due to the absence of a harbor for mooring, fishermen resort to mooring inside Damietta Nile branch, which leads to pollution of the River Nile from the remnants of fishing boats. Thus, the numerical CMS is applied in this research to investigate the effects of multiple layout scenarios on sedimentation within the proposed Ezbet Elborg fishing harbor by constructing a database of 100 scenarios. Using this date set, an effective model is developed to help in evaluating and predicting harbors' sedimentation quantities to choose the optimum conceptual planning of harbors aiming at mitigating the adverse impacts of sedimentation issues.

## 3. Research methodology

### 3.1. Numerical data source

In this research, one hundred scenarios are simulated numerically using CMS to determine the relationship between the volume of sedimentation inside a harbor basin and the corresponding harbor layout with various breakwater parameters. CMS is developed in 2006 by the Coastal Inlets Research Program (CIRP) to provide an accurate and reliable representation of coastal processes affecting the operation and maintenance of coastal inlet structures such as jetties and breakwaters, as well as in the risk assessment of shipping in inlets and harbors [34]. CMS is a combined suite of two-dimensional (2DH) modules for flow, waves, and sediment transport with morphological changes that has shown to be an effective numerical tool for calculating the sedimentation quantities of harbors [14]. Usually, before using numerical models for simulating specific issues, those models should be firstly calibrated by quantitatively measuring the agreement between predictions provided by the model and field observations representing the real world. For CMS model calibration, bathymetry evolution maps (October 2014 and October 2015) are used. The CMS model is provided by a measured wave data by S4DW gauge, water surface elevation (WSE) data from tide gauge, current measurements, and sediment characteristics. Then, the model runs based on a steering module (the CMS-Flow model coupled with the CMS-Wave model) to predict the bottom evolution after one-year starting from October 2014 to October 2015. Numerous profiles distributed along the study area were investigated for calibration purposes. A sample of investigated profiles is shown in Fig. 2. The results confirm the accuracy of the model and demonstrate that the model can be used to simulate the coastal processes in the study area and predict the sedimentation quantities with an average correlation coefficient ($R^2 = 0.97$) between modeled and real values of the bathymetry for the investigated profiles.

After conducting the calibration of the CMS model, the proposed scenarios are performed by continually changing the design parameters (Fig. 3): Length of the first part of the main breakwater ($L_1$), Angle of the first part of the main breakwater ($\alpha_1$), Length of the second part of the main breakwater ($L_2$), Angle of the second part of the main breakwater ($\alpha_2$), Length of the secondary breakwater ($L_3$), Angle of the secondary breakwater ($\alpha_3$), Harbor basin width (B), Rock diameter (D) and Porosity (n). Within the harbor basin, a polygon is drawn in which the monthly accumulated sedimentation volume ($V_s$) for each scenario is estimated at the end of

**Table 1**
Statistical analysis of the resulted CMS inputs and output.

| **Inputs** | | | | | | | | | | **Output** |
|---|---|---|---|---|---|---|---|---|---|---|
| **Scenario No** | $L_1$ | $\alpha_1$ | $L_2$ | $\alpha_2$ | $L_3$ | $\alpha_3$ | **B** | **n** | **D** | **Vs** |
| **Unit** | **m** | **Degree** | **m** | **degree** | **m** | **degree** | **m** | **---** | **m** | **m$^3$** |
| **Mi** | 800 | 30 | 400 | 30 | 600 | 30 | 150 | 0.2 | 1.5 | 18,350 |
| **Mx** | 1000 | 80 | 800 | 80 | 800 | 80 | 200 | 0.4 | 2 | 49,500 |
| **M** | 932 | 57 | 620 | 69.35 | 785 | 47.15 | 189 | 0.281 | 1.63 | 30,022 |
| **SD** | 79 | 14.4 | 77.8 | 17.7 | 45.8 | 18.3 | 20.8 | 0.1 | 0.2 | 8,445 |
| **Sk** | -0.6 | 0.5 | -1 | -1.3 | -3.1 | 0.5 | -1.3 | 0.2 | 1 | 0.5 |

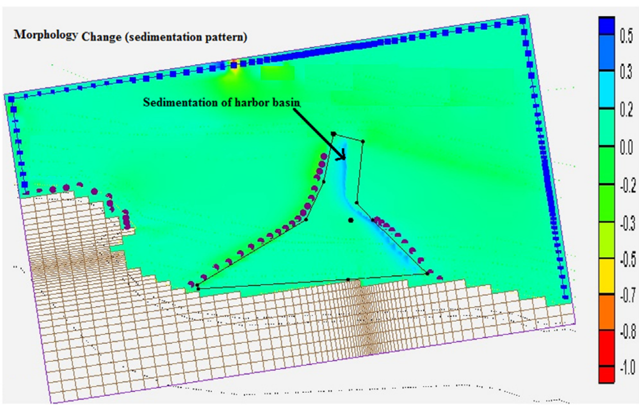


**Fig. 4.** Sample of sedimentation pattern for one scenario (side bar: erosion/accretion in (m)).

the simulation as shown in Fig. 4 and the recorded data are presented in Table A in supplementary materials.

Moreover, it should be noticed that the prevailing wave direction is almost from North-North-West (NNW) which resulted in bypassing sediment at the entrance of the harbor and deposited behind the secondary breakwater as shown in Figs. 3 and 4.

To better understand the actions of each input parameter towards the *Vs*, a correlation heatmap matrix is executed and automated by utilizing the MATLAB APPs toolbox to illustrate the relationship between the various variables as outlined in Fig. 5. As clearly shows in Fig. 5, no powerful positive or negative linear correlation between any pair of variables which reflects that the prediction of the sedimentation is a very complex process with multiple variables associated with high nonlinearity and stochasticity. In this case, the physical models and conducting numerical modeling require hundreds of CPU hours, both solutions seem to be time-consuming and costly. The implementation of AI models will, therefore, make a significant contribution by better modeling the sedimentation process.

Herein, data investigation is performed using statistical indicators such as mean (M), maximum (Mx), minimum (Mi), standard deviation (SD), and the skewness (Sk) of variables. Table 2 summarizes the statistical analysis for the dataset used in this study. Fig. 6 presents the data distribution of all variables. As per this investigation and the results presented in Table 1 and Fig. 6, the following remarks are drawn:

§ $(\alpha_1)$, $(\alpha_3)$, $(n)$ and $(V_s)$ having lower skewness values which indicate that the data can be considered normally distributed.
§ $(L_1)$, $(L_2)$, $(D)$, $(\alpha_2)$, $(B)$ and $(D)$ have an average skewness value which indicate that they are moderately skewed.

Generally, through the performed statistical analysis, most of the inputs, except $(L_3)$ are well distributed and suitable for the training of the AI models.

Here, to model $V_s$, the obtained data was standardized using Eq. (1). Furthermore, data standardization assures a zero-centered distribution of all variables to provide effective data processing [35].

$$\mathcal{Z} = \left(\frac{x-\mu}{\sigma}\right) \tag{1}$$

Where, $\mathcal{Z}$ is the scaled value of the unscaled variable x with a mean $(\mu)$ and a standard deviation $(\sigma)$. Lastly, the gathered data set (100 scenarios) was divided into 70% as training data and 30% as testing data. The testing data will be used to evaluate the developed model to ensure its robustness.

### *3.2. Proposed models*

#### *3.2.1. Support Vector Regression (SVR)*

SVR is a computational intelligence approach applied mathematical learning theory that can be used for both regression classification and tasks [20]. In SVR, the regression problem can be expressed using Eq. (2).

$$y = f(x) = \sum_{i=1}^{n} w \times K(X_i \,.\, X) + b. \tag{2}$$

Where w is the weight vector, b is the bias factor, n is the size of the data set, and $K(X_i \,.\, \mathrm{X})$ is the Kernel function. Internal parameters values are calculated using the least square method by decreasing the regularized risk function as expressed below:

$$\text{Minimize} = \mathrm{R(C)} : \frac{1}{2}\|w\|2 + C\sum_{i=1}^{n}(\xi_i + \xi_i^*) \tag{3}$$

subjected to $y_i$ $(w \times x_i + b) \geq 1\text{-}\xi_i$ where $\xi_i \geq 0$ & $C > 0$.

Where C is a weighing parameter that is assumed to determine a trade-off between empiric risk and model flatness, $(\xi_i)$ and $(\xi_i{}^*)$ are slack variables that represent the distance from the real values to the corresponding boundary values. The objective of the SVR is to minimize $(\xi_i)$ and $(\xi_i^*)$ and $\|w\|^2$. Several Kernel-function formulations can be used in the SVR algorithm. In the present study, three Kernel functions (Linear, Polynomial, and Radial basis) are investigated via a trial-and-error technique to choose the best one based on their performance. The formulations of the utilized Kernel functions are presented in Eqs. (4)–(6).

$$\text{Linear (homogeneous)} K(X_i.\mathrm{X}) = X_i X, \tag{4}$$

$$\text{Polynomial } K(X_i.\mathrm{X}) = (X_i X + 1)^d, \tag{5}$$

$$\text{Radial basis } K(X_i.\mathrm{X}) = exp\left(C(\|X_i \,\mathrm{X}\|)^2\right). \tag{6}$$

Where, $X_i.X$ are the training and test patterns, $d$ represents the degree of polynomial and $(C \leq 0)$ are Kernel parameters.

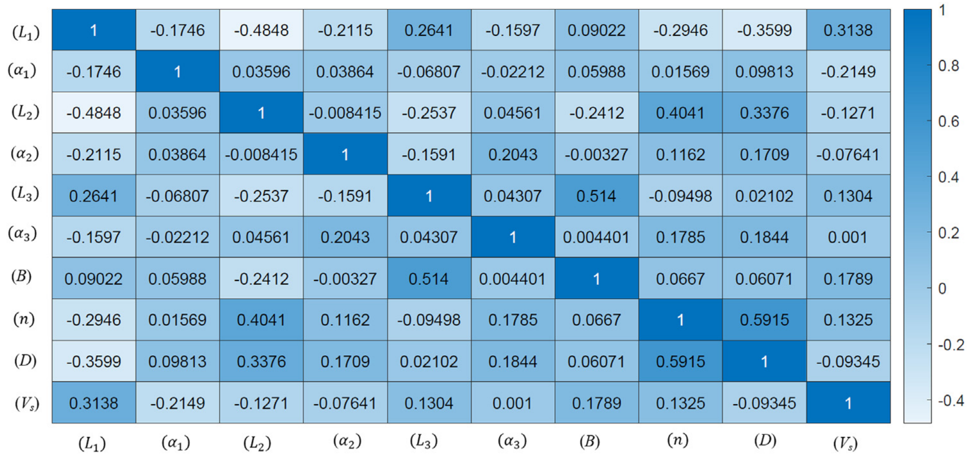


**Fig. 5.** Correlation analysis between input and output variables.

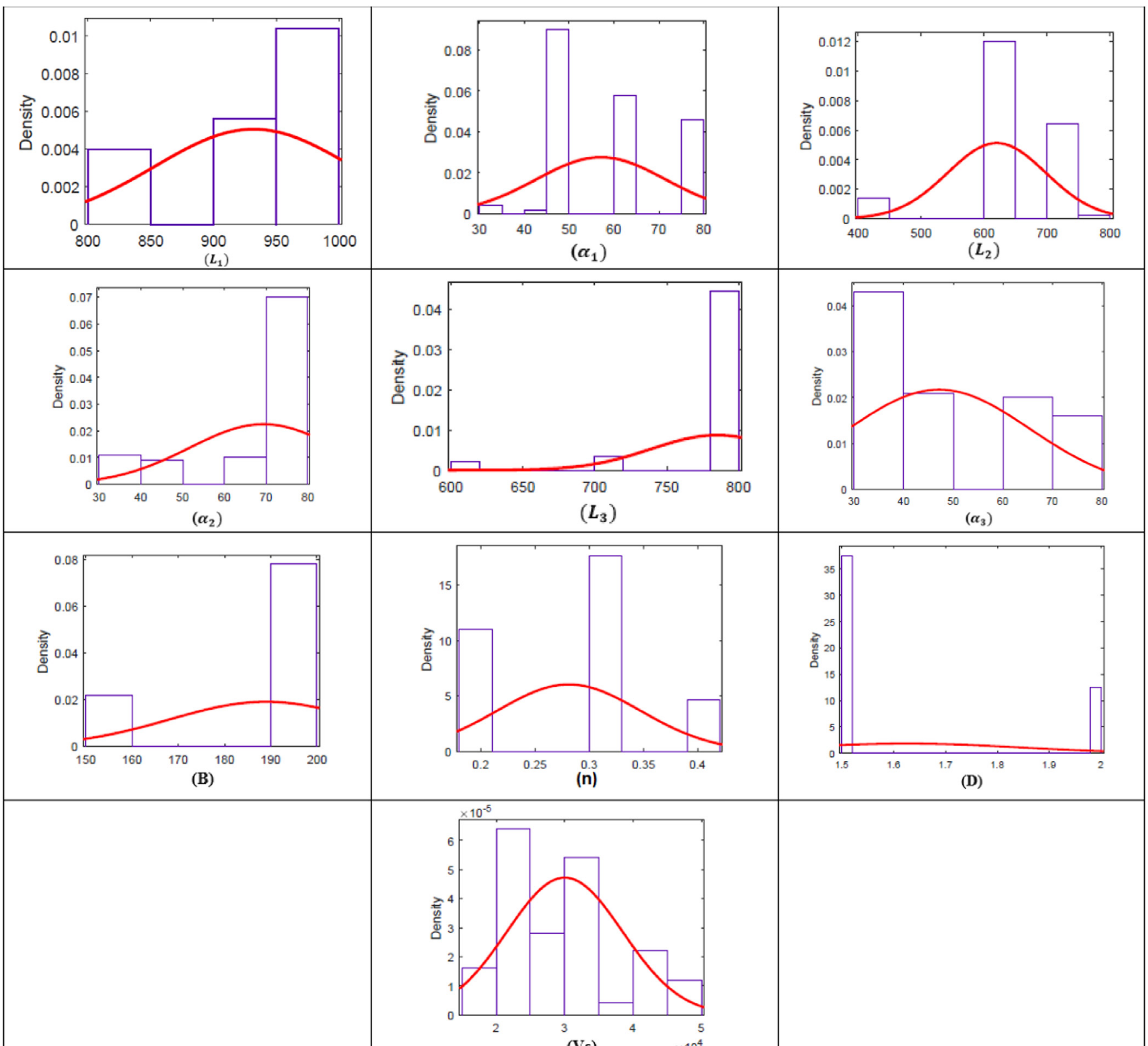


**Fig. 6.** Distribution plot of input and output variables.

*3.2.2. Gaussian Processing Regression (GPR)*

GPR is a non-parametric AI technique, as it does not predict the realistic essence of the simulation system [36,37]. GPR key benefits are the interpretability of prediction and results, and the probabilistic nature when embedding any preceding models [36–38]. Theoretical work and real-world implementation have shown over the last few decades that GPR is an effective method for supervised learning applications [38]. For a training set $D = [(x_i.y_i).i\ =\ 1.\ \ldots\ .n]$, the input data $X \in R^{D*n}$ is called the dataset matrix and $y \in R^n$ is the desired output vector. The main assumption of the GPR is that the output $y$ can be estimated as:

$$y_i = f(x_i) + \varepsilon_i. \tag{7}$$

where $\varepsilon_i$ is the Gaussian noise with variance $(\sigma_n^2)$. In the Gaussian process, the signal term $f(x)$ is often considered a random variable.

$$f(x_i) = \mathcal{GP}\left[m(x).:\ K\left(x.x'\right)\right] \tag{8}$$

Where $m(x)$ is a mean function which often set to 0, and $K\left(x - x'\right)$ is a covariance function which explains previous assumptions, such as probable smoothness of data and trends. Then, the joint probabilistic Gaussian distribution of the training outputs $y$ and the predicted function $f*$ can be written as:

$$\begin{bmatrix} y \\ f^* \end{bmatrix} = \mathcal{N}\left(0.\begin{bmatrix} K(X.X) + \sigma_n^2 I_n & K(X.x_*) \\ K(X.x_*) & K(x_*.x_*) \end{bmatrix}\right). \tag{9}$$

Where, $I_n$ is an identity matrix, $\sigma_n^2$ is the assumed variance of training samples, and $K(X.x_*)$ is a matrix of the evaluated covariance in all pairs of test and training data sets that are similar for other values of $K(X, x*)$, $K(x*, X)$, and $k(x*, x*)$, in which $X$ is training, while $x*$ is the test data.

Herein, four covariance functions named Quadratic (squared), exponential, squared exponential and Matern are used to select the most appropriate one, those functions can be expressed as:

$$\text{Quadratic (squared)}\quad K\left(x\ .x'\right) = \left(1 + \left(\frac{(x - x')}{2\lambda}\right)^2\right), \tag{10}$$

$$\text{Exponential}\ K\left(x\ .x'\right) = exp\left(1 + \left(\frac{(x - x')}{2\lambda}\right)^2\right) \tag{11}$$

$$\text{Squared exponential}\ K\left(x\ .x'\right) = \sigma_n^2\ exp\left(1 + \left(\frac{(x - x')}{2\lambda}\right)^2\right), \tag{12}$$

$$\text{Matern}\ K\left(x\ .x'\right) = \sigma^2 K_m\left(\sqrt{\left[\sum_{i=1}^{n}\frac{x_i^2}{\lambda_i^2}\right]}\right). \tag{13}$$

where $\sigma^2$ controls the prior variance, $\lambda$ is an isotropic length scale parameter and $K_m$ is the one-dimensional Matern covariance function.

*3.2.3. ANN model*

ANN is a very useful AI tool for the solution of problems caused by the inability of the manual solution when the data are too much [39]. There are various types of neural networks including the feed-forward back propagation neural network (FFBPNN), the cascade-forward back propagation neural network (CFNN), and generalized regression neural network (GRNN) [40]. However, many studies have shown that FFBPNN is capable of producing close approximation to any continuous nonlinear mapping type of problems [41,42]. The general ANN system consists of three layers: input (variables), hidden (functional layer), and output layers (network's response) [40]. Those layers are composed of several basic computing components called neurons; this may be presented as follow:

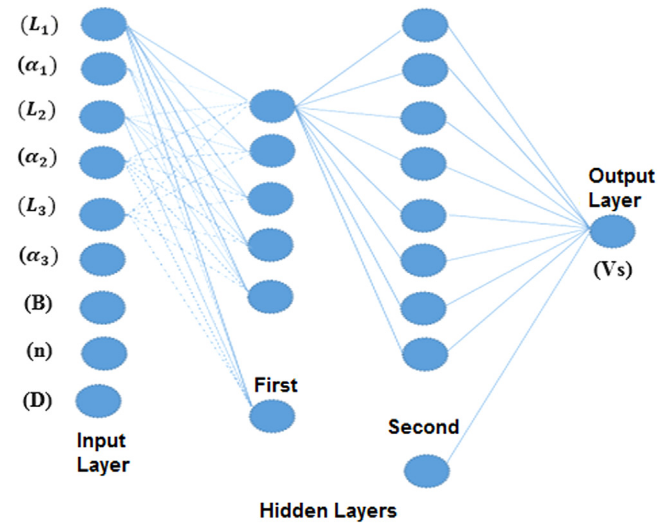


**Fig. 7.** Architecture of the proposed ANNs model for modeling Vs.

$$Y = f\left(\sum_{i=1}^{n} w_i x_i + b\right). \tag{14}$$

Where $Y$ is the neuron's output; $x_i = x_1, x_2, ...., x_n$ are the input values; $w_i = w_1, w_2, ...., w_n$ are the connection weights; $b$ is the bias value; and $f$ is the activation function. In this process, the collected test data from experiments are multiplied by weights and transferred to the activation function. There are various activation functions can be utilized in ANNs such as linear, tangent sigmoid, and radial basis [40]. In the present work, as recommended by Bakr and Negm [43], the common sigmoid function is utilized as the activation function of the signal for the neuron in the hidden layer as follows:

$$Y = f(x) = \frac{1}{1 + e^{-x}}. \tag{15}$$

Additionally, after training, the BP algorithm measures the error, then adjusts the weights, first for the output layer, and then distributes it back to hidden and input layers. Eventually, a linear transformation function is utilized in the output layer to predict the $V_s$.

Each stage of any ANN modeling involves trial and error experiments to create an effective and stable network. There is no standardized rule for choosing the correct number of hidden layers and the corresponding number of neurons in each layer. Thus, iterative procedures are used in this work to increase the number of neurons in one and two hidden layers and measuring the network performance. Fig. 7 displays the proposed ANN architecture for this study.

*3.3. Models' evaluation*

Different statistical metrics are used to evaluate the model's capability. Among those are, the RMSE, the CC and the SI. These metrics are expressed as follows [44–46]:

$$RMSE = \sqrt{\frac{1}{n}\sum_{i=1}^{n}(P_i - O_i)^2}, \tag{16}$$

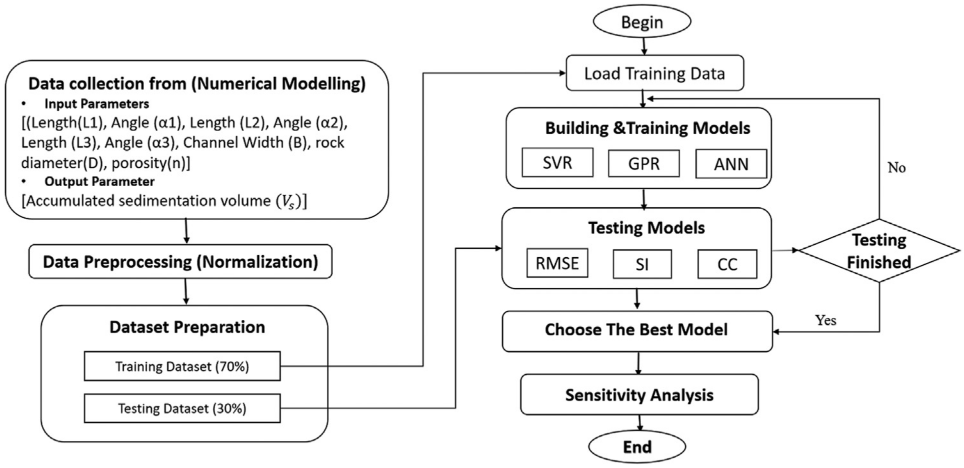


**Fig. 8.** Research methodology.

**Table 2**
SVR models with statistical measures.

| SVR Kernel function | | Training Data | | | Testing Data | | |
|---|---|---|---|---|---|---|---|
| | | RMSE ($m^3$) | SI | CC | RMSE ($m^3$) | SI | CC |
| **Linear (homogeneous)** | | 6,540 | 0.14 | o.41 | 6,953 | 0.15 | 0.32 |
| **Polynomial** | **Quadratic** | 2,840 | 0.08 | 0.91 | 3,237 | 0.09 | 0.85 |
| | **Cubic** | **1,350** | **0.07** | **0.98** | **2,215** | **0.06** | **0.95** |
| **Radial basis function** | | 2,350 | 0.07 | 0.94 | 2,710 | 0.08 | 0.91 |

$$CC = \frac{\sum_{i=1}^{n} \left(P_i - \bar{P}\right)\left(O_i - \bar{O}\right)}{\sqrt{\sum_{i=1}^{n} \left(P_i - \bar{P}\right)^2 \sum_{i=1}^{n} \left(O_i - \bar{O}\right)^2}}, \tag{17}$$

$$SI = \frac{RMSE}{\bar{O}}. \tag{18}$$

where $(O_i)$, $(P_i)$ are the observed and predicted values, $n$ is the number of datasets, $(\bar{P})$, $(\bar{O})$ are the mean values of observation and predictions, respectively.

Finally, Fig. 8 presents a summary of the proposed research methodology that used in this study to estimate the $V_s$. The MATLAB software and related packages are used to train and test the developed AI models.

## 4. Results and discussion

### 4.1. Proposed models evaluation

In SVR, different Kernel functions are trained and evaluated to fine-tune the heuristics of the SVR models. Table 2 compares the statistical measures values estimated using train and test data for different SVR models to determine the Support Vector Genius (SVG). The SVG is the model with the minimum error and the most precision when determining the validation set's target value. Linear Kernel function shows low generalization efficiency compared to all SVR models (CC Training = 0.41 and CC Testing = 0.32) in prediction of the $V_s$ with SI= 0.14 and 0.15 for training and testing data, respectively. It is also apparent that the model with the highest approximation is the one with the cubic Kernel function with CC= 0.98 and 0.95 for the training and testing, respectively.

As the same in SVR, four covariance GPR functions are used to determine Gaussian Processing Genius (GPG). Table 3 presents the kernel functions' results. From the Table, it can be concluded that the change between covariance functions doesn't improve the model accuracy significantly. Even though, the model with the

**Table 3**
GPR models with statistical measures.

| GPR covariance function | Training Data | | | Testing Data | | |
|---|---|---|---|---|---|---|
| | RMSE ($m^3$) | SI | CC | RMSE ($m^3$) | SI | CC |
| **Quadratic (squared)** | 2750 | 0.08 | 0.93 | 3,090 | 0.09 | 0.87 |
| **Exponential** | 2710 | 0.08 | 0.93 | 3,069 | 0.09 | 0.88 |
| **Squared exponential** | 2750 | 0.08 | 0.93 | 3,090 | 0.09 | 0.87 |
| **Matern** | **2690** | **0.08** | **0.93** | **3,020** | **0.09** | **0.88** |

Matern covariance function is slightly better than other GPR models with CC Training = 0.93 and CC Testing = 0.88.

For modelling $V_s$ through ANN, different scenarios were designed and evaluated. The optimum model structure is presented in Fig. 7. The initial ANN scenario is constructed with one input layer representing the nine input parameters, one hidden layer started with 10 neurons and output layer of one node, $V_s$. To design a stable FFBPNN, a parametric analysis is performed by changing the number of neurons in the hidden layers (one layer and two hidden layers are checked) as presented in Table B in supplementary materials. From Table B, it can be concluded the results of ANN scenarios are very close in the training dataset (CC is more than 94%). Also, the same can be seen in the testing stage. Thus, the structure of the best model obtained is (9-16-14-1), namely, a network with nine input variables, sixteen neurons for the first hidden layer and fourteen neurons for the second hidden layer with a single output (see Fig. 7).

From these results, the estimated regression best configuration criterion for the SVR, GPR and ANN models for the training and testing cases is presented in Table 4. It is concluded that the ANN model performs better than both the SVR and the GPR models in predicting $V_s$. The performance of the AI models is also illustrated with scatter plots (Fig. 9). Fig. 9 demonstrates the relationship between the sedimentation observed and predicted using the CC. The results reveal that the ANN outperforms the other models. Moreover, the Taylor diagram, presented in Fig. 10, is a practical tool

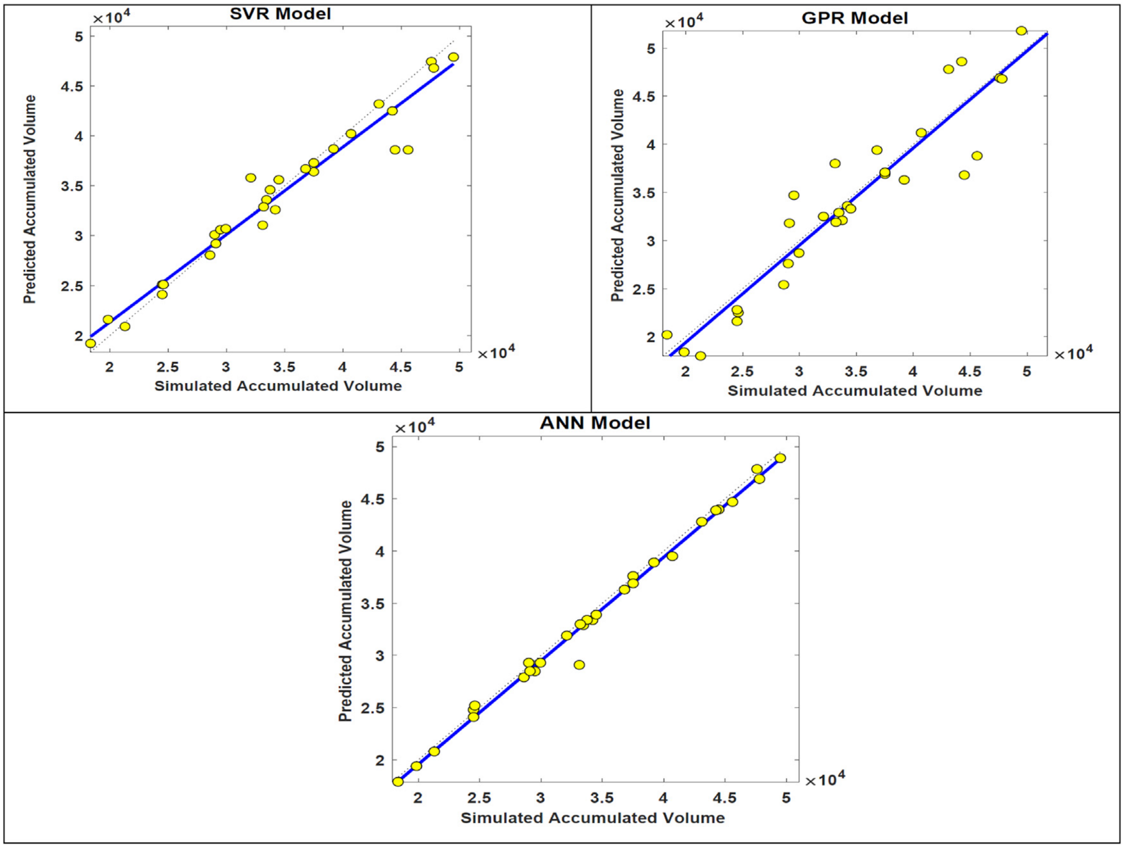


**Fig. 9.** Performance of the developed AI models.

**Table 4**
Statistical measures for the optimal proposed AI models.

| Model | Training Data | | | Testing Data | | |
|---|---|---|---|---|---|---|
| | RMSE | SI | CC | RMSE | SI | CC |
| **SVR (cubic)** | 1350 | 0.07 | 0.98 | 2215 | 0.06 | 0.95 |
| **GPR (Matern)** | 2690 | 0.08 | 0.93 | 3020 | 0.09 | 0.88 |
| **ANN (9-16-14-1)** | 910 | 0.03 | 0.99 | 930 | 0.03 | 0.99 |

for better understanding the potential of the developed different models. The diagram provides a descriptive overview of the predicted and observed accreted volume according to several statistical parameters, including RMSE, standard deviations and CC. In the Taylor diagram, the most accurate model is explained by the point with the lower RMSE and higher R values. Therefore, the Taylor diagram proves that the ANN model is superior to the other models.

### 4.2. Validation of ANN model

To validate the ANN model, ten scenarios different from the previous scenarios used in training and testing stages are randomly selected and extracted numerically from the CMS for validation purposes. The mean absolute percentage error (MAPE), in Eq. (19), is used for evaluating the models' performance according to the criteria shown in Table. 5.

$$MAPE = \frac{1}{n}\sum_{i=1}^{n}\frac{P_i - O_i}{O_i} * 100 \tag{19}$$

The calculated $V_s$ from the numerical CMS simulation model and from the developed ANN model are presented in Table. 6. Based on the computed values of the MAPE = 4% and CC = 0.94

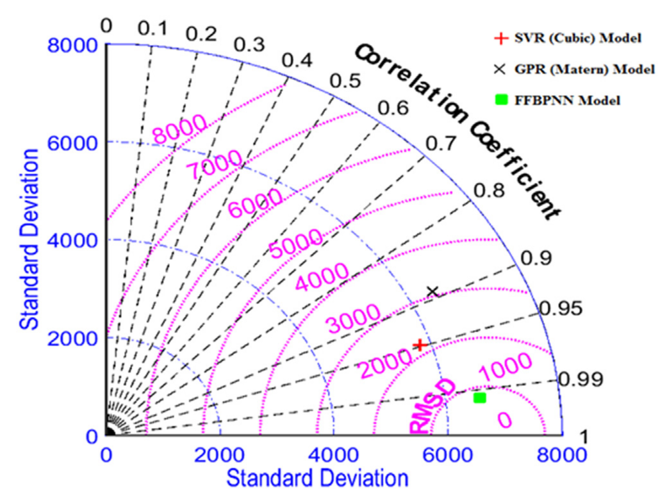


**Fig. 10.** Taylor diagram for the performance of the developed AI models in the testing phase.

between the two models; this reveals the ability of the proposed model to accurately predict the $V_s$.

### 4.3. Sensitivity analysis

To minimize the data space if an input variable is discovered that does not influence the final outcomes of the forecast, the impact of input variables is evaluated. The key concept is to successively exclude one input variable from the input space while at the same time keeping the others at their median values. The approach thus helps one to measure how sensitive a model is to individual

**Table 5**
Rating criteria of MAPE [47].

| Category No | MAPE (%) | Strength of predication |
|---|---|---|
| 1 | <10 | High |
| 2 | 10 – 20 | Good |
| 3 | 20 – 50 | Reasonable |
| 4 | > 50 | Inaccurate |

parameters of the data. Pointedly, a new nine-dimensional input space is constructed using the previously developed ANN model based on the distribution of the probability density of each variable. All input parameters are successively excluded from the input space by setting the column to zero values. MATLAB feature selection criteria are used to measure the effect of each parameter.

From Table 7, it is observed that the highest mean RMSE obtained is 5,561 m$^3$ for the angle of the first part of the main breakwater ($\alpha_1$) when excluded from the prediction process, with lowest mean (CC) value of 0.57. That means that it is difficult to achieve the acceptable performance of the ANN prediction model without ($\alpha_1$) in the input space. Thus, ($\alpha_1$) is the most significant input variable for the sedimentation volume prediction. The second and third important input factors in the prediction process are the porosity (n), with CC = 0.68 and RMSE = 4,860, and the channel width (B), with CC = 0.71 and RMSE = 4,620 m$^3$. Also, the length of the first part of the main breakwater ($L_1$), and the angle of the secondary breakwater ($\alpha_3$) have a significant impact on the performance of the ANN model.

Additionally, in this research, the output solution deviation or sensitivity level ($\theta_i$) according to the CC is as follow:

$$\theta_i = \frac{O_i - O_{ref}}{O_{ref}} . \tag{20}$$

Where ($O_i$) is the output (CC) when the input (i) is excluded, $O_{ref}$ is the output (CC) for the predication process when the variables were kept at their median value. According to the level of sensitivity analysis, which is presented in Fig. 11, although most of the parameters are effective on the ANN output, the ($\alpha_1$), ($n$) and ($B$) are the most important parameters in the input space. The current results are consistent with the results obtained from previous physical models, which verified that the inclination of the main breakwater, basin width, and breakwater porosity are the main contributors to sediment deposition within the harbors' basin [2,10].

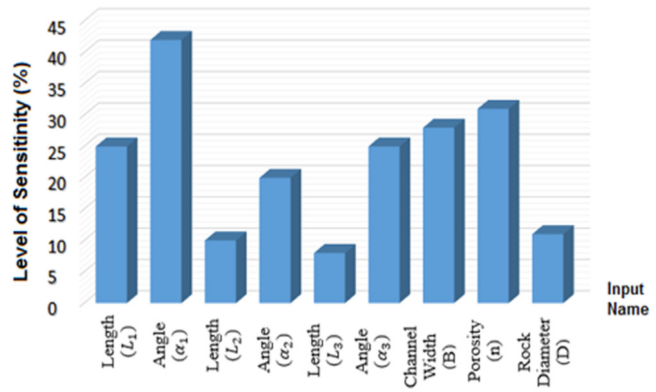


**Fig. 11.** Sensitivity analysis according to the CC value of the proposed ANN model.

### 4.4. Managerial and practical contribution

Harbors' Authorities in developing countries don't have sufficient resources or funding for the construction of physical models. In addition, those models require huge effort, much time, and high costs. Thus, the available numeric data opens unprecedented opportunities for AI algorithms as a compensate tool for better evaluation and prediction of harbors' sedimentation quantities. As such, this research attempted to address this deficiency in resources, funding, and staff by developing a data-driven decision support tool that could be used by the Egyptian harbors' authorities to evaluate and predict the sedimentation in harbors' basins. For this purpose, a user-friendly interface is developed (using MATLAB APPs Designer) to facilitate the designer/modeler to calculate the predicted accumulated sedimentation volume without experience with modeling and simulation tools (Fig. 12) based on the proposed ANN model. This graphical user interface (GUI) offers the user several alternative choices depending on the input parameters describing the model.

The developed GUI is a graphical representation consisting of buttons and icons on the left side at which the user can easily insert the inputs data as shown on the right side. Then, by pressing the "Calculate" button, the monthly volume of sedimentation can be calculated.

In conclusion, the AI framework developed in this paper has many practical contributions which can be summarized as follows: (1) The developed decision-making tool possesses many benefits compared to physical models of harbors including: ease of implementation, accuracy, automation, customizability, scalability, speed, time-cycle reduction and inexpensive. (2) The gathered information based on the sensitivity analysis of the developed AI model for estimation of the harbors' sedimentation quantities and the factors that significantly impact the sedimentation volume could create new knowledge on existing inadequacy of presently used approaches which lead to enhanced harbors' planning. (3) The proposed AI framework could be utilized as a predictive maintenance tool and thus helps to set enhanced strategies for maintenance. Furthermore, the decision tool developed in this paper is thought to be unique, since there are no similar research works in the literature.

**Table 6**
The $V_s$ values from both the CMS and the FFBPNN models.

| **Inputs** | | | | | | | | | | $V_s$ (m$^3$) | |
|---|---|---|---|---|---|---|---|---|---|---|---|
| **Sec No** | $L_1$ | $\alpha_1$ | $L_2$ | $\alpha_2$ | $L_3$ | $\alpha_3$ | **B** | **n** | **D** | **CMS** | **ANN** |
| **Sc1** | 900 | 45 | 600 | 80 | 800 | 30 | 200 | 0.4 | 2 | 43,630 | 42,510 |
| **Sc2** | 900 | 30 | 600 | 80 | 800 | 45 | 200 | 0.4 | 2 | 34,230 | 36,440 |
| **Sc3** | 900 | 30 | 600 | 45 | 800 | 30 | 200 | 0.3 | 1.5 | 33,420 | 29,590 |
| **Sc4** | 1000 | 80 | 500 | 45 | 800 | 30 | 200 | 0.4 | 2 | 42,340 | 39,040 |
| **Sc5** | 1000 | 45 | 500 | 60 | 800 | 30 | 200 | 0.4 | 2 | 38,980 | 39,240 |
| **Sc6** | 800 | 45 | 500 | 60 | 800 | 45 | 200 | 0.3 | 1.5 | 34,250 | 33,820 |
| **Sc7** | 1000 | 45 | 500 | 80 | 800 | 30 | 150 | 0.4 | 2 | 44,750 | 42,620 |
| **Sc8** | 800 | 45 | 500 | 80 | 800 | 30 | 150 | 0.4 | 2 | 29,640 | 30,370 |
| **Sc9** | 1000 | 45 | 600 | 80 | 800 | 30 | 150 | 0.3 | 2 | 46,100 | 45,410 |
| **Sc10** | 900 | 45 | 800 | 80 | 800 | 30 | 200 | 0.4 | 2 | 40,630 | 40,590 |

**Table 7**
Sensitivity analysis of the input parameters with respect to the CC and RMSE.

| Input | $L_1$ | $\alpha_1$ | $L_2$ | $\alpha_2$ | $L_3$ | $\alpha_3$ | B | n | D |
|---|---|---|---|---|---|---|---|---|---|
| **RMSE ($m^3$)** | 4375 | 5561 | 2753 | 3833 | 2600 | 4370 | 4620 | 4860 | 2877 |
| **CC** | 0.74 | 0.57 | 0.89 | 0.79 | 0.91 | 0.74 | 0.71 | 0.68 | 0.88 |

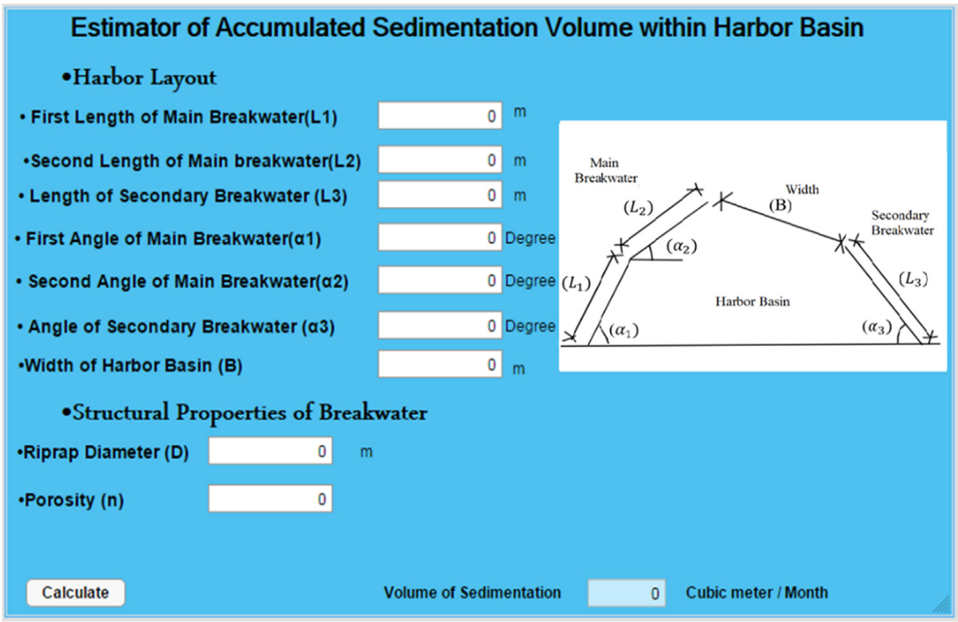


**Fig. 12.** The GUI for calculating sedimentation within a harbor basin.

## 5. Conclusions

Predicting sedimentation in harbors' basins is one of the most complex processes since it is correlated with several variables characterized by stochasticity nature. The main goal of this work is to develop an AI data-driven decision support tool that can reliably predict harbors' sedimentation quantities. Accordingly, a total of 100 scenarios of sedimentation behaviour gathered numerically from the CMS and used to generate the training and testing datasets for the AI models. Out of these, a total of nine input variables including harbor's layout and breakwater parameters with the volume of accumulated sedimentation as the prediction target were used in the modelling. SVR, GPR and ANN are proposed and evaluated. Overall, the ANN with CC = 0.99 outperforms other models. To further investigate the role of each individual input variable in the developed model, a detailed sensitivity analysis was carried out. It was found that ($\alpha_1$), ($n$) and ($B$) are the most significant input parameter for the sedimentation prediction. In general, this study contributes to the coastal structures' management by devising a data-driven framework which expected to help engineers to select the suitable design parameters of harbors' basins and quickly be able to predict the harbors' sedimentation quantities. Further, the authorities responsible for the management of harbors' are recommended to utilize the developed decision support tool during the conceptual planning of harbors because no cost is associated with its implementation which contributes to enhancing maintenance dredging strategies associates with the sedimentation issues.

While the present study revealed significant advances in predicting and modelling the sedimentation issue, the limitation should not be overlooked. The main shortage of this research is that it's only applicable to fishing harbors that are located on the Mediterranean's sea study areas with similar environmental field conditions. However, the used approach can be adapted to other study areas with different environmental and geometrical characteristics. Furthermore, the authors seek to incorporate the developed ANN model with an evolutionary algorithm technique to build an optimization model for calculating the optimized design harbors' layout and breakwater parameters to achieve both the environmental and economic goals.

## Declaration of Competing Interest

The authors declare no conflict of interest.

## Acknowledgments

This work was supported by the National Research Foundation of Korea (NRF) grant funded by the Korea government (MSIT) (NRF-2021R1A2B5B02002599).

## Supplementary materials

Supplementary material associated with this article can be found, in the online version, at doi:10.1016/j.joes.2022.06.005.

## References

[1] O.E. Frihy, E.A. Deabes, E.E.D.F. Helmy, J. Coast. Res. 32 (3) (2016) 555, doi:10.2112/JCOASTRES-D-14-00181.1.
[2] M. Mojabi, K. Hejazi, M. Karimi, Int. J.MAr.Sci.Eng 3 (2) (2013) 57–68.
[3] H. Li, L. Lin, C.C. Lu, and A.T. Shak, 2011, pp. 2585–2598, 10.1142/9789814355537_0194.
[4] M. Zikra, S. Salsabila, K. Sambodho, Fluids 6 (11) (2021) 397, doi:10.3390/FLUIDS6110397.
[5] A.M.G.S. Ferreira, C.S.N. Santos, Sediment. Eng. (2018), doi:10.5772/INTECHOPEN.74049.
[6] Z. Demirbilek, et al., Investigation of Shoaling in the Federal Navigation Channel, Illinois Coastal and Hydraulics Laboratory, Waukegan Harbor, 2020.

[7] J. Yin, R.A. Falconer, Y. Chen, S.D. Probert, Appl. Energy 67 (3) (2000) 341–352.
[8] J.C. Winterwerp, J. Waterw. Port Coast. Ocean Eng. 131 (6) (2005) 258–266, doi:10.1061/(ASCE)0733-950X(2005)131:6(258).
[9] C. Kuijper, H. Christiansen, J.M. Cornelisse, J.C. Winterwerp, J. Waterw. Port Coast. Ocean Eng. 131 (6) (2005) 267–276, doi:10.1061/(ASCE)0733-950X(2005)131:6(267).
[10] Ö. Yüksek, J. Waterw. Port Coast. Ocean Eng. 121 (1) (1995) 13–22, doi:10.1061/(ASCE)0733-950X(1995)121:1(13).
[11] O. Stoschek, C. Zimmermann, J. Waterw. Port Coast. Ocean Eng. 132 (5) (2006) 410–414, doi:10.1061/(ASCE)0733-950X(2006)132:5(410).
[12] L.C. Van Rijn, Int. J. 20 (1) (2005) 39–51.
[13] F. Sakhaee, F. Khalili, J. Ocean Eng. Sci. 6 (1) (2021) 70–84, doi:10.1016/J.JOES.2020.04.002.
[14] R. Styles, M.E. Brown, K.E. Brutsché, H. Li, T.M. Beck, A. Sánchez, J. Mar. Sci. Eng. 4 (4) (2016) 65, doi:10.3390/jmse4040065.
[15] B.L. Meena, J.D. Agrawal, Proced. Eng. 116 (1) (2015) 607–614, doi:10.1016/j.proeng.2015.08.332.
[16] V. Nourani, A. Hosseini Baghanam, J. Adamowski, O. Kisi, J. Hydrol. 514 (2014) 358–377, doi:10.1016/j.jhydrol.2014.03.057.
[17] Y. Huang, J. Li, J. Fu, CMES Comput. Model. Eng. Sci. 121 (3) (2019) 845–875 Tech Science Press, doi:10.32604/cmes.2019.07653.
[18] M. Ashphaq, P.K. Srivastava, D. Mitra, J. Ocean Eng. Sci. 6 (4) (2021) 340–359, doi:10.1016/j.joes.2021.02.006.
[19] A.N. Deshmukh, M.C. Deo, P.K. Bhaskaran, T.M. Balakrishnan Nair, K.G. Sandhya, IEEE J. Ocean. Eng. 41 (4) (2016) 944–953, doi:10.1109/JOE.2016.2521222.
[20] S.G. Patil, S. Mandal, A.V. Hegde, Adv. Eng. Softw. 45 (1) (2012) 203–212, doi:10.1016/j.advengsoft.2011.09.026.
[21] A. Molajou, V. Nourani, A. Afshar, M. Khosravi, A. Brysiewicz, Water Resour. Manag. 35 (8) (2021) 2369–2384, doi:10.1007/S11269-021-02818-2.
[22] M.K. Sen, S. Dutta, G. Kabir, N.N. Pujari, S.A. Laskar, J. Clean. Prod. 288 (2021), doi:10.1016/J.JCLEPRO.2020.125526.
[23] A. Golmohammadi, S. Bonab, A. Parishani, Int. J. Ind. Eng. Comput. 7 (3) (2016) 481–488.
[24] V. Nourani, M.T. Sattari, A. Molajou, Water Resour. Manag. An Int. J. Publ. Eur. Water Resour. Assoc. 31 (9) (2017) 2645–2658, doi:10.1007/S11269-017-1649-Y.
[25] A.B. Da'ie, Int. J. Innov. Res. Sci. Stud. 4 (2) (2021) 133–138, doi:10.53894/IJIRSS.V4I2.68.
[26] A.O. Elfaki, O.A. Abouabdalla, S.L. Fong, G.M.D. Johar, K.L.O.O.T. Aik, R. Bachok, J. Theor. Appl. Inf. Technol. 42 (1) (2012) 75–93.
[27] G. Yin, et al., Arab. J. Chem. 15 (3) (2022) 103612, doi:10.1016/J.ARABJC.2021.103612.
[28] L. Zajmi, F.Y.H. Ahmed, A.A. Jaharadak, Appl. Comput. Intell. Soft Comput. 2018 (2018) 1–7, doi:10.1155/2018/9547212.
[29] A.A.M. Alwreikat, H. Rjoub, S. Afr. J. Bus. Manag. 51 (1) (2020) 11, doi:10.4102/SAJBM.V51I1.2046.
[30] S. Jafarian-Namin, A. Goli, M. Qolipour, A. Mostafaeipour, A.M. Golmohammadi, Int. J. Energy Sect. Manag. 13 (4) (2019) 1038–1062, doi:10.1108/IJESM-06-2018-0002/FULL/PDF.
[31] A.M. Golmohammadi, M. Honarvar, H. Hosseini-Nasab, R. Tavakkoli-Moghaddam, Fuzzy Inform. Eng. 12 (2) (2020) 204–222, doi:10.1080/16168658.2020.1747162.
[32] A.A. Dodaran, P.S. Kil, J. Ocean Eng. Sci. 4 (2) (2019) 149–165, doi:10.1016/j.joes.2019.03.003.
[33] M. Samy, A. Mahmoud, Study for Improving Efficiency of Egyptian Fishing Ports, Egypt-Japan University of Science and Technology (E-JUST), 2018.
[34] C.W. Reed, M.E. Brown, A. Sánchez, W. Wu, A.M. Buttolph, J. Coast. Res. SPEC. ISSUE. 59 (2011) 1–6 SPEC. ISSUEMar., doi:10.2112/SI59-001.1/27079/THE-COASTAL-MODELING-SYSTEM-FLOW-MODEL-CMS-FLOW.
[35] D.R. Vincent, N. Deepa, D. Elavarasan, K. Srinivasan, S.H. Chauhdary, C. Iwendi, Sensors 19 (17) (2019) 3667 (Switzerland), doi:10.3390/s19173667.
[36] S.A. Aye, P.S. Heyns, Mech. Syst. Signal Process. 84 (2017) 485–498, doi:10.1016/j.ymssp.2016.07.039.
[37] E. Schulz, M. Speekenbrink, A. Krause, J. Math. Psychol. 85 (2018) 1–16, doi:10.1016/j.jmp.2018.03.001.
[38] S.L. Jiang, X. Shen, Z. Zheng, Processes 7 (6) (2019), doi:10.3390/pr7060352.
[39] W.S. Alaloul, A.H. Qureshi, Dyn. Data Assim. (2020).
[40] The Mathworks Inc., ⟨13:italic ⟩www.mathworks.com/products/matlab⟨/13:italic⟩, 2016.
[41] Y. Zhang, D. Guo, Z. Li, IEEE Trans. Neural Netw. Learn. Syst. 24 (4) (2013) 579–592, doi:10.1109/TNNLS.2013.2238555.
[42] O.I. Abiodun, et al., IEEE Access 7 (2019) 158820–158846, doi:10.1109/ACCESS.2019.2945545.
[43] M.H. Bakr, M.H. Negm, in: Advances in Imaging and Electron Physics, 174, Academic Press Inc., 2012, pp. 223–260.
[44] M.R. Kaloop, A.R. Gabr, S.M. El-Badawy, A. Arisha, S. Shwally, J.W. Hu, Front. Struct. Civ. Eng. 13 (6) (2019) 1379–1392, doi:10.1007/s11709-019-0562-2.
[45] M.R. Kaloop, S.M. El-Badawy, J. Ahn, H.-B. Sim, J.W. Hu, R.T. Abd El-Hakim, Int. J. Pavement Eng. (2020) 1–15, doi:10.1080/10298436.2020.1776281.
[46] M. Kumar, A. Bardhan, P. Samui, J.W. Hu, M.R. Kaloop, Processes 9 (3) (2021) 486, doi:10.3390/pr9030486.
[47] J.J. Montaño Moreno, A. Palmer Pol, A. Sesé Abad, B. Cajal Blasco, Psicothema 25 (4) (2013) 500–506, doi:10.7334/psicothema2013.23.